*Erschienen in: Cell Chemical Biology ; 26 (2019), 11. - S. 1535-1543.e5*
*https://dx.doi.org/10.1016/j.chembiol.2019.08.004*

# Formation of the Alarmones Diadenosine Triphosphate and Tetraphosphate by Ubiquitin- and Ubiquitin-like-Activating Enzymes

**Kathrin H. Götz,[1] Martin Mex,[1] Katrin Stuber,[1,2] Fabian Offensperger,[2] Martin Scheffner,[2] and Andreas Marx[1,3,*]**
[1]Department of Chemistry, Konstanz Research School Chemical Biology, University of Konstanz, Universitätsstrasse 10, 78464 Konstanz, Germany
[2]Department of Biology, Konstanz Research School Chemical Biology, University of Konstanz, Universitätsstrasse 10, 78464 Konstanz, Germany
[3]Lead Contact
*Correspondence: andreas.marx@uni-konstanz.de

## SUMMARY

**Diadenosine polyphosphates ($Ap_nAs$) such as diadenosine tri- and tetraphosphates are formed in prokaryotic as well as eukaryotic cells. Since upon stress intracellular $Ap_nA$ concentrations increase, it was postulated that $Ap_nAs$ are alarmones triggering stress-adaptive processes. The major synthesis pathway of $Ap_nAs$ is assumed to be a side reaction of amino acid activation. How this process is linked to stress adaptation remains enigmatic. The first step of one of the most prominent eukaryotic post-translational modification systems—the conjugation of ubiquitin (Ub) and ubiquitin-like proteins (Ubl) to target proteins—involves the formation of an adenylate as intermediate. Like $Ap_nA$ formation, Ub and Ubl conjugation is significantly enhanced during stress conditions. Here, we demonstrate that diadenosine tri- and tetraphosphates are indeed synthesized during activation of Ub and Ubls. This links one of the most prevalent eukaryotic protein-modification systems to $Ap_nA$ formation for the first time.**

## INTRODUCTION

Diadenosine polyphosphates ($Ap_nAs$) are a class of nucleotides found in prokaryotes and eukaryotes (Farr et al., 1989). They consist of two adenosine moieties that are linked by a polyphosphate consisting of a variable number of phosphates via phosphoester bonds to the respective 5′-OH group. Although $Ap_nAs$ were reported as early as the 1960s, their physiological role remains mostly elusive (Zamecnik et al., 1966). In multicellular organisms, $Ap_nAs$ are found in intra- and extracellular environments. Whereas extracellular $Ap_nAs$ have been associated with several regulatory functions, such as the regulation of the cardiovascular system (Flores et al., 1999), platelet aggregation (Luthje et al., 1985), and insulin-secretory activity (Verspohl and Johannwille, 1998), the functions of intracellular $Ap_nAs$ are poorly understood. They have been linked to cell proliferation, as different $Ap_nA$ concentrations have been observed in different cell-cycle phases (i.e., reaching peak concentrations in S phase) (Baker and Jacobson, 1986; Moris et al., 1987; Rapaport and Zamecnik, 1976). However, other results question the role of $Ap_nAs$ in cell proliferation (Baxi and Vishwanatha, 1995; McLennan, 2000; Moris et al., 1987; Weinmann-Dorsch et al., 1984). Furthermore, upon exposure to different stress signals (e.g., oxidative stress, heat, UV irradiation) (Baker and Jacobson, 1986; Garrison et al., 1986; Karras et al., 2014; McLennan, 1992), $Ap_nA$ concentrations rose from nano- up to micromolar concentrations, whereas the concentration of ATP was found to not change significantly (Baker and Jacobson, 1986; Garrison et al., 1986; Karras et al., 2014; McLennan, 1992). As this suggests that $Ap_nAs$ are involved in cellular stress and damage-response pathways, they were termed "alarmones" (McLennan, 2000). Diadenosine triphosphate ($Ap_3A$), for example, has significant impact on the activity of the human fragile histidine triad protein (Fhit). Fhit is the main hydrolase of $Ap_3A$, cleaving it to AMP and ATP (Barnes et al., 1996; Thorne et al., 1995). Furthermore, the short-lived Fhit/$Ap_3A$ complex is associated with tumor-suppressor activity (Siprashvili et al., 1997) by representing the starting point of a signal transduction pathway toward apoptosis (Campiglio et al., 2006; Saldivar et al., 2010). Accordingly, dysregulated expression of the Fhit protein has been observed in various types of cancer including gastrointestinal (Dagmar et al., 1997), kidney (Huebner et al., 1997), breast (Bianchi et al., 2007), lung (Sozzi et al., 1997), and cervical (Hendricks et al., 1997) carcinomas.

Diadenosine tetraphosphate ($Ap_4A$) has been studied extensively in the context of the DNA-damage response. Treatment of cells with non-cytotoxic doses of mitomycin C, a DNA cross-linking agent, leads to a significant increase in $Ap_4A$ concentrations (Marriott et al., 2015). Furthermore, it was reported that $Ap_4A$ levels are elevated when DNA-repair proteins such as X-ray repair cross-complementing protein 1 (XRCC1) or ADP-ribosyltransferase diphtheria toxin-like 1 (ARTD1) are absent and that they are restored to normal levels upon re-expression of these enzymes (Marriott et al., 2015). Similarly, increasing $Ap_4A$ concentrations have been associated with stalled replications forks to allow DNA repair (Marriott et al., 2015; McLennan, 2000; Varshavsky, 1983). If the extent of DNA damage reaches a certain threshold the level of $Ap_4A$ remains high, which can result

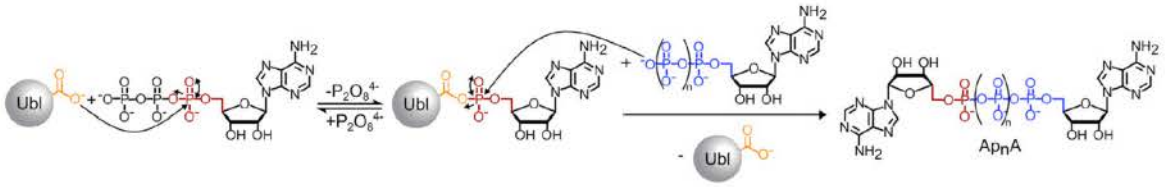


**Figure 1. Hypothetical Model of $Ap_nA$ Synthesis by the Ubiquitin-Activating Enzyme E1**

Ubiquitin (Ub) and ubiquitin-like proteins (Ubl) are C-terminally adenylated by their cognate Ub/Ubl-activating enzymes E1 under consumption of ATP. In order for $Ap_nA$ synthesis to occur, the adenylate is attacked by the phosphate group of an additional ADP/ATP (n = 1, 2) molecule, resulting in the formation of $Ap_3A$/$Ap_4A$ (n = 1, 2), respectively, and free E1.

in cell death via apoptosis (Vartanian et al., 1997, 1999, 2003). In addition, it has been shown that cells in which the gene encoding the $Ap_4A$ hydrolase Nudix (nucleoside diphosphate linked to X) type motive 2 (*NudT2*) is disrupted exhibit high levels of $Ap_4A$. Concurrently, they display a downregulation of inflammatory and innate immune responses (Marriott et al., 2016), indicating that $Ap_4A$ may be involved in transcriptional regulation.

To add another layer of complexity, it has been shown that not only the absolute concentrations of $Ap_3A$ and $Ap_4A$ determine the cellular response, but also that their ratio ($Ap_3A$/$Ap_4A$) is an important determinant of the cellular fate (Vartanian et al., 1997, 1999, 2003). However, it is still unknown how cells fine-tune $Ap_3A$ and $Ap_4A$ levels (Marriott et al., 2015).

$Ap_4A$ formation was originally discovered (Zamecnik et al., 1966) while studying the process of charging bacterial $^{Lys}$tRNA with L-lysine by the lysyl-tRNA synthetase *in vitro*. Indeed, to date the main route of $Ap_nA$ synthesis is believed to be a side reaction of the aminoacyl-tRNA synthetase (aaRS)-catalyzed activation of amino acids for loading onto tRNAs (Brevet et al., 1989; Guo et al., 2009; Plateau and Blanquet, 1982; Zamecnik et al., 1966). This reaction proceeds via the following steps (Goerlich et al., 1982). First, aminoacyl-AMP is formed, which is then attacked by the 3′ end of the cognate tRNA to form the correctly loaded aminoacyl-tRNA or alternatively by a nucleotide (ADP/ATP) to form $Ap_3A$ or $Ap_4A$, respectively (Goerlich et al., 1982). Since in most cases the presence of the cognate tRNA inhibits $Ap_nA$ synthesis (Kisselev et al., 1998), aaRS that require the respective tRNA as cofactor for aminoacyl-AMP synthesis (e.g., argRS, glnRS, gluRS) are not capable of $Ap_nA$ formation (Kisselev et al., 1998). The formation efficiency of different $Ap_nA$s depends on the specific aaRS, but $Ap_4A$ is usually the predominant product (McLennan, 1992).

It is well established that cellular stress is accompanied by global downregulation of protein biosynthesis (Clemens, 2001; Proud, 2005; Shenton et al., 2006). This is mediated by several mechanisms including the degradation of the cellular tRNA pool (Sorensen et al., 2017; Thompson et al., 2008), which may result in increased $Ap_nA$ synthesis by aaRSs. Besides aaRS, the only other mammalian enzyme that has been shown to synthesize $Ap_nA$ *in vitro* is the DNA ligase IIIβ/DNA ligase IIIα (Fontes et al., 1998; Fraga and Fontes, 2011; McLennan, 2000; Sillero and Sillero, 2000). The common mechanistic feature of these enzymes is the formation of an adenylate intermediate. The degree to which the different reactions contribute to $Ap_nA$ synthesis is unknown (Fraga and Fontes, 2011; McLennan, 2000). In addition, it was speculated that other enzymes, which also catalyze reactions with adenylates as intermediates and which are known to be active during the cellular stress response, might contribute to the dynamics of the cellular $Ap_nA$ pool (Fraga and Fontes, 2011; McLennan, 1992).

Upon stress, a significant increase of proteins modified by ubiquitin (Ub) (Aiken et al., 2011; Finley et al., 1987; Wang et al., 2010) and/or by the ubiquitin-like proteins (Ubl) SUMO (Impens et al., 2014) and NEDD8 (Leidecker et al., 2012) is observed. These modifications direct proteins to different fates, including proteasomal degradation and alteration of subcellular localization, and thereby contribute to the elicitation of cellular responses that are crucial to maintain or re-establish cellular homeostasis (Park and Ryu, 2014). Notably, the E1 Ub-/Ubl-activating enzymes (e.g., UBA1 for Ub), which catalyze the first step of the Ub/Ubl enzymatic cascade, form a Ub/Ubl-adenylate intermediate (Figure 1) (Komander and Rape, 2012; Spasser and Brik, 2012; Swatek and Komander, 2016; Varshavsky, 2017). Since the formation of adenylate intermediates appears to be crucial for the enzymatic synthesis of $Ap_nA$ (Atencia et al., 1999; Fontes et al., 1998; Goerlich et al., 1982; Madrid et al., 1998; Sillero and Sillero, 2000; Zamecnik et al., 1966), we hypothesized that E1s may also have the ability to synthesize $Ap_nA$ (Figure 1). In this case, the adenylated Ub/Ubl would react with an ATP or ADP molecule to form $Ap_4A$ or $Ap_3A$, respectively, instead of reacting with the active-site cysteine residue of the E1, which promotes the further Ubl cascade.

Here, we investigated the potential formation of $Ap_nA$ by E1 enzymes by analysis of the reaction products by high-performance liquid chromatography coupled to high-resolution mass spectrometry (HPLC-HRMS). We found that $Ap_nA$s are formed as by-products during Ub and Ubl activation by the respective E1 enzymes. The influence of different E2 Ub-conjugating enzymes on the E1-mediated reaction was studied as well, revealing that with increasing E2 concentrations $Ap_nA$ synthesis decreased. Our results unambiguously show that Ub/Ubl E1s are capable of producing $Ap_nA$s, linking one of the most ubiquitous eukaryotic protein-modification systems to $Ap_nA$ formation.

## RESULTS AND DISCUSSION

### Quantification of $Ap_3A$ or $Ap_4A$ Levels

To investigate whether E1 enzymes are a potential source of $Ap_nA$ formation (Figure 1), we first established an analytical method that allows reliable quantification of $Ap_3A$ and $Ap_4A$ levels. To do so, we decided to employ HPLC-HRMS. In brief, the HPLC conditions were first optimized using mononucleotides

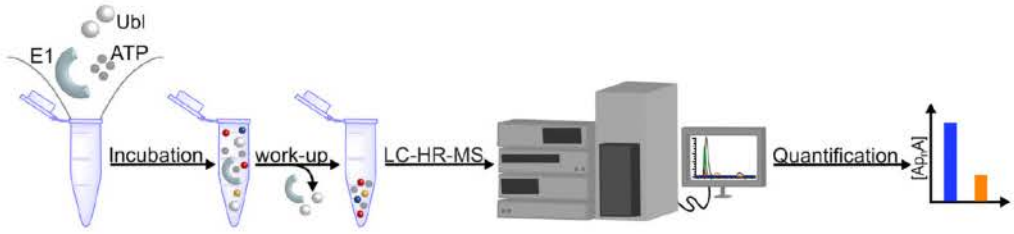


**Figure 2. General Method for Detection of $Ap_nA$ Synthesis by E1 Enzymes**

ATP, Ub/Ubl, and the respective E1 enzyme are incubated in reaction buffer. The reaction is stopped after a certain time by cooling to 0°C. After workup (i.e., removal of E1 and Ub/Ubl), the nucleotide species of the reaction mixture are analyzed and quantified by HPLC-HRMS.

(AMP, ADP, ATP) and dinucleotides ($Ap_3A$, $Ap_4A$) as reference samples to ensure that retention times of the mononucleotides and dinucleotides are significantly different (Figure S1). This enabled the unequivocal detection of the $Ap_nAs$ as well as their quantification by HRMS with a detection limit of 2.0 pmol $Ap_nA$ in 20 μL. The detection limit was determined in probes containing an equimolar mixture of $Ap_3A$ and $Ap_4A$. Furthermore, we ensured that the sample workup and, especially, the extraction efficiency during protein removal is high. In the lower micromolar range, which is of particular importance for our application, over 98% of the respective nucleotide was recovered and quantified by the established HPLC-HRMS-based method (see Figure S1).

## Formation of $Ap_4A$ by UBA1

After optimization of the analytical procedure, formation of $Ap_nAs$ during activation of Ub by UBA1 was investigated by the workflow shown in Figure 2. A mixture of Ub and ATP was incubated with increasing concentrations of UBA1 (0.5–2.0 μM) at 37°C (Figure 3). After 12 h, the reactions were stopped by cooling to 0°C. Following workup (i.e., removal of Ub and UBA1 by $ZipTip_{C4}$ pipette tips), the nucleotide species present in the reaction mixtures were analyzed by HPLC-HRMS (Figure 3A). In reactions where UBA1 and/or Ub were omitted (Figure 3A' #1–3), $Ap_4A$ synthesis was not detectable. Starting from 0.5 μM UBA1 up to 2.0 μM UBA1, an increasing $Ap_4A$ concentration ranging from 1.1 ± 0.1 μM to 4.1 ± 0.1 μM was observed. Of note, the concentrations of Ub, UBA1, and ATP are within the range that has been described for their cellular concentrations (Manfredi et al., 2002; Siepmann et al., 2003; Traut, 1994).

Since in the presence of 0.8 μM UBA1, $Ap_4A$ was detected with sufficient signal-to-noise ratio (Figures 3A and 3D), this concentration was chosen for all subsequent experiments. Note that our results are in contrast to an earlier report, in which $Ap_4A$ formation by UBA1 was not observed (Günther Sillero et al., 2005). There might be various reasons for this, since the experimental setups differ in several regards. For example, we used an HPLC-HRMS-based analysis technique that is likely to be more sensitive than the readout employed previously (combination of thin-layer chromatography and autoradiography). Also, the source of UBA1 and the reaction conditions were different.

We also determined $Ap_4A$ levels relative to the AMP generated that represents the final product of UBA1-mediated activation of Ub. As expected, the AMP concentration increased only when UBA1 was present (Figure 3B, #3–11). Furthermore, the reaction containing UBA1 but in the absence of Ub (Figure 3B, #3) showed only a minor increase in AMP concentration, indicating some background activity of the enzyme. In reactions where UBA1, Ub, and ATP were present (Figure 3B, #4–11), significant synthesis of AMP as well as of $Ap_4A$ was observed. We found that the detected $Ap_4A$ concentration is about 20% of the AMP concentration (Figures 3B and S1).

In addition, we investigated the time dependency of the reaction. Processing and analysis of the samples revealed that $Ap_4A$ was formed in a time-dependent manner, with the highest $Ap_4A$ concentration observed after 12 h (Figure S2). Furthermore, besides analysis by HRMS, the identity of $Ap_4A$ was confirmed by enzymatic cleavage of the reaction products. For this purpose, the $Ap_4A$ phosphorylase Rv2613c of *Mycobacterium tuberculosis* that specifically cleaves $Ap_4A$ was added to the reaction mixture (Götz et al., 2017; Mori et al., 2011). Indeed, we found that in all reactions containing Rv2613c, $Ap_4A$ could no longer be detected (Figure S2) unlike the cleavage products ATP and ADP.

## Mechanism of $Ap_4A$ Synthesis by UBA1

To gain insight into the mechanism of UBA1-mediated $Ap_4A$ formation, we employed mutants of UBA1 and Ub, respectively. We investigated UBA1-C632S, in which the active-site cysteine residue is replaced by serine. Therefore, Ub-adenylate formation can still take place (as measured by AMP formation; see Figure S2), but not the subsequent step of Ub activation, i.e., Ub cannot be transferred from the adenylate to the active-site cysteine via thioester bond formation (Groen and Gillingwater, 2015). Furthermore, we employed the ubiquitin variants Ub-G76M, in which the C-terminal glycine at position 76 is replaced by methionine, and Ub-His, in which the C terminus of Ub is modified with a polyhistidine tag (His6x). Both Ub modifications prevent C-terminal adenylation by UBA1 (Hershko and Ciechanover, 1998). In addition, the variants Ub-R72A and Ub-LIA were investigated, since they have altered interaction properties toward UBA1. Ub-R72A exhibits a lower affinity to UBA1, especially when it is adenylated (Burch and Haas, 1994). In the LIA (L8A, I44A) variant, the so-called canonical hydrophobic patch of Ub is affected (Schafer et al., 2014). This patch is, among other features, directly involved in the interaction of Ub with UBA1, i.e., mutation of this patch results in general in a weaker interaction between Ub and UBA1 (Schafer et al., 2014). Reactions were performed in the absence and presence of the respective mutated and wild-type proteins and analyzed as described above.

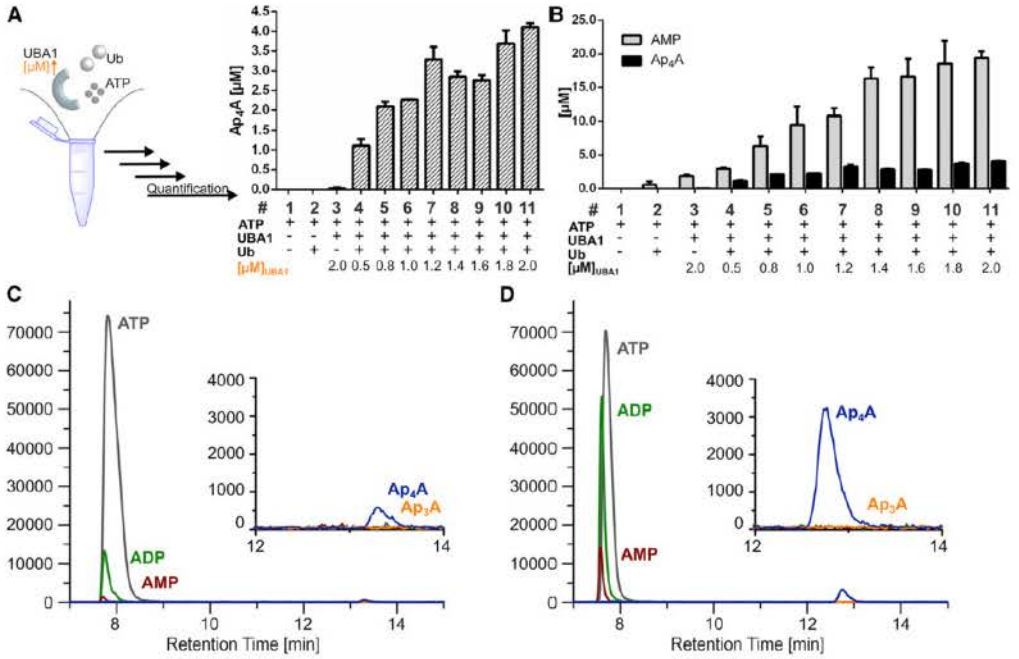


**Figure 3. The Ubiquitin-Activating Enzyme UBA1 Catalyzes the Formation of $Ap_4A$**

(A) Synthesis of $Ap_4A$ by UBA1 in an enzyme concentration-dependent fashion. Increasing amounts of UBA1 (0.5–2.0 µM) were incubated with 60 µM Ub and 1 mM ATP in reaction buffer. Reactions without UBA1 and/or Ub served as controls. All reactions were incubated for 12 h at 37°C. Thereafter, reactions were stopped by cooling to 0°C. After workup, nucleotide species were analyzed by HPLC-HRMS. Note that commercially available ATP (measured in sample #1) contains $Ap_4A$. Accordingly, the respective concentration was subtracted from the $Ap_4A$ concentrations measured in the various samples. All data represent mean ± standard error of triplicates.

(B) Comparison of the AMP and $Ap_4A$ concentrations shows that ~20% of the ATP consumed results in $Ap_4A$ formation. All data represent mean ± standard error of triplicates.

(C) Representative extracted ion chromatogram (EIC) traces of sample #2 (i.e., control reaction in the absence of Ub and UBA1).

(D) Exemplary EIC traces of sample #6.

In reactions containing either UBA1-C632S (Figure 4A, #5 and #6) or a Ub variant that cannot be adenylated (Ub-G76M and Ub-His; Figure 4B, #5–8) synthesis of $Ap_4A$ was not observed. Likewise, no $Ap_4A$ synthesis was detected when the interaction between UBA1 and Ub was weakened (Ub-LIA, Ub-R72A; Figure 4B, #9–12). Only reactions containing both wild-type proteins, which allow efficient adenylate as well as thioester formation, resulted in detectable $Ap_4A$ synthesis (Figures 4A and 4B, #4). Taken together, the data suggest that both active sites of UBA1 (i.e., adenylate formation, thioester complex formation) must be occupied for $Ap_4A$ synthesis to occur (see also Figure 7).

## Synthesis of $Ap_4A$ in the Presence of Ub-Conjugating Enzymes

We next investigated the effect of Ub-conjugating (E2) enzymes (Stewart et al., 2016) (UbcH5b, UbcH1) on $Ap_4A$ synthesis, since they accept Ub from UBA1 by transthioesterification and may thus have a negative effect on $Ap_4A$ synthesis. To test this hypothesis, we added increasing amounts of the E2s to the reaction mixture containing UBA1, Ub, and ATP (final ratios of UBA1/E2 = 1:1, 1:2, 1:5, and 1:11; Figure 5). Indeed, we observed that the presence of E2s decreases $Ap_4A$ formation, with UbcH1 affecting $Ap_4A$ synthesis more pronouncedly than UbcH5b (Figure S3). With increasing concentrations of UbcH1, $Ap_4A$ formation was almost completely suppressed, showing a significant effect ($p < 0.05$) at a UBA1/E2 ratio of 1:5 (Figure 5B, #8). At a UBA1/UbcH5b ratio of 1:1, a significant increase ($p < 0.05$) of $Ap_4A$ concentration was detectable (Figure 5C, #6); this might be due to the described UBA1-stimulating effect of UbcH5b (Ciechanover, 1998; Hacker et al., 2013). With further increasing concentrations of UbcH5b, $Ap_4A$ formation decreases with a significant effect ($p < 0.05$) at the highest UBA1/UbcH5b ratio (1:11; Figure 5C, #9).

Concerning the $Ap_4A$:AMP ratio in reactions containing E2 enzymes (Figure S3), the ratio decreases with increasing E2 enzyme concentration, i.e., AMP concentration increases with a concomitant decrease in $Ap_4A$ concentration. The increase of AMP is in line with the described UBA1-stimulating effect of E2 enzymes (Ciechanover, 1998; Hacker et al., 2013). As described above for $Ap_4A$ formation, UbcH1 had a more pronounced effect on AMP formation than UbcH5b (Figure S3), indicating that UbcH1 was more active in accepting Ub from UBA1 than UbcH5b (Hacker et al., 2013). Therefore, the different effects of the E2s on $Ap_4A$ synthesis are most likely due to variations in activity.

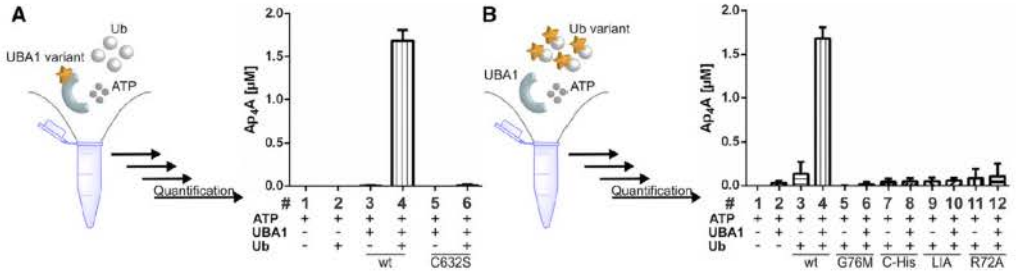


**Figure 4. Characterization of UBA1-Mediated $Ap_4A$ Synthesis**

(A) Investigation of wild-type UBA1 (UBA-wt) and its variant UBA1-C632S. The reaction mixture contained 0.8 µM UBA1-C632S or UBA1-wt, 60 µM Ub, and 1 mM ATP in reaction buffer. Reactions without UBA1-C632S and/or Ub as well as the reaction with UBA1-wt served as controls (#1–4).

(B) Investigation of Ub and its variants Ub-G76M, Ub-His, Ub-LIA, and Ub-R72A. The reaction mixtures contained 0.8 µM UBA1, 60 µM Ub variant, and 1 mM ATP in reaction buffer. Reactions without UBA1 and/or Ub variants as well as the reaction with Ub-wt served as controls (#1–5, 7, 9, 11). All reactions (A and B) were incubated for 12 h at 37°C. Thereafter, the reactions were stopped by cooling to 0°C. After workup, the nucleotide species were analyzed by HPLC-HRMS. The $Ap_4A$ concentration that is present in commercially available ATP (as measured in sample #1 in A and B) was subtracted from the $Ap_4A$ concentrations detected in the different samples. Mutants of UBA1 and Ub are indicated. All data represent mean ± standard error of triplicates.

## Synthesis of $Ap_3A$ by UBA1

During incubation of the reaction mixtures at 37°C, we observed that ADP was formed to a concentration of 10–30 µM, presumably due to spontaneous hydrolysis of ATP. However, formation of $Ap_3A$—which in principle could be generated by nucleophilic attack of the Ub-adenylate by ADP—was not detected by HPLC-HRMS in any of the experiments described above. To determine whether higher concentrations of ADP can lead to $Ap_3A$ formation, we incubated increasing ADP concentrations (up to a final concentration of 1.0 mM) with UBA1, Ub, and ATP. Indeed, with increasing concentrations of ADP we detected increasing $Ap_3A$ formation while $Ap_4A$ formation decreased (Figure S4), yet the amounts of $Ap_3A$ formed were approximately 8- to 10-fold lower than those found for $Ap_4A$ in the absence of ADP (Figure S4). Furthermore, we found that the presence of 5 mM ADP or higher inhibits the UBA1-catalyzed formation of both $Ap_3A$ and $Ap_4A$ (Figure S5). It is likely that ADP at such high concentrations acts as a competitive inhibitor of UBA1, preventing adenylate formation in general.

## Formation of $Ap_nA$ by the Activating Enzymes of NEDD8 and SUMO

Activation of the Ubl proteins NEDD8 and SUMO proceeds via a mechanism analogous to the activation of Ub (Bohnsack and Haas, 2003; Kerscher et al., 2006; Lois and Lima, 2005). Thus, we next investigated whether the respective E1 enzymes also catalyze $Ap_nA$ formation.

As shown in Figure 6, $Ap_4A$ synthesis was indeed detected for both Ubl-activating enzymes. The amount of $Ap_4A$ synthesized by the NEDD8-activating enzyme (NAE) (Figure 6C) was slightly lower than that formed in reactions containing UBA1 (UBA1: 2.1 ± 0.1 µM versus NAE: 1.4 ± 0.1 µM). Using the SUMO-activating enzyme (SAE) (Figure 6D), one-tenth of the amount synthesized by UBA1 (0.2 ± 0.03 µM) was formed. However, the AMP concentration generated, which represents the final product of the E1-mediated activation of the respective Ubl and thus serves as a measure for E1 activity, is comparable for all investigated E1 enzymes (Figure S6). This suggests that UBA1 is more active in $Ap_4A$ formation than NAE and, in particular, SAE. As for UBA1, synthesis of $Ap_3A$ could not be observed for NAE or SAE under the conditions used (not shown).

## Potential mechanism of $Ap_nA$ synthesis by Ub/Ubl-activanting enzymes E1

As shown in Figure 3, the concentration of $Ap_4A$ formed by UBA1 in the absence of E2 enzymes is about 20% of the amount of AMP that is released from the Ub-adenylate during transthioesterification. In the presence of E2, however, the formation of $Ap_4A$ is diminished (Figure 5). Furthermore, by employing defined UBA1 and Ub variants, we discovered that only reactions containing both wild-type proteins, which allow efficient adenylate as well as thioester formation, result in detectable $Ap_4A$ synthesis (Figure 4). The fact that adenylate as well as thioester formation are important for $Ap_4A$ synthesis suggests the following mechanistic model for the E1-promoted $Ap_4A$ synthesis (Figure 7). First, a Ub molecule is activated by UBA1 at the expense of ATP by adenylate formation (Figure 7, 1–2) and subsequent transfer to the active-site cysteine resulting in a thioester linkage (Figure 7, 3). A second Ub is then adenylated by UBA1 under consumption of a second ATP (Figure 7, 4–5) (Komander and Rape, 2012; Spasser and Brik, 2012; Swatek and Komander, 2016; Varshavsky, 2017). This is the state in which the side reaction leading to $Ap_4A$ formation mainly occurs (Figure 7, 6a). The adenylate is attacked by the phosphate group of an additional ATP molecule, resulting in the formation of $Ap_4A$ and free Ub as well as UBA1-S-Ub, which can enter the catalytic cycle again (Figure 7, 7).

## SIGNIFICANCE

**In this study, we investigated the potential of Ub/Ubl E1 activating enzymes to form $Ap_4A$ and $Ap_3A$. To study $Ap_nA$ formation, we established a sensitive HPLC-HRMS-based quantification method. Indeed, using this analytical technique we discovered and quantified $Ap_4A$ formation during Ub/Ubl activation. By adding ADP to the reaction (up to 1.0 mM), $Ap_3A$ synthesis was also observed. However,**

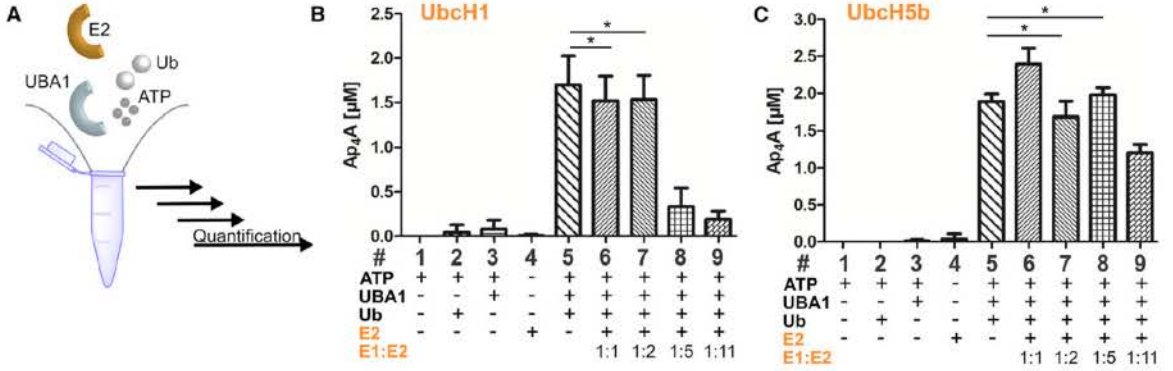


**Figure 5. Effect of E2 Ubiquitin-Conjugation Enzymes on UBA1-Mediated $Ap_4A$ Synthesis**

(A) Synthesis of $Ap_4A$ by UBA1 in the presence of different concentrations of Ub-conjugating enzymes E2 (UbcH1 [B] and UbcH5b [C]).The reaction mixture contained 0.8 µM UBA1, 60 µM Ub, 1 mM ATP, and the respective E2 enzyme in reaction buffer. Ratios of the respective E2 enzyme to UBA1 are indicated. Reactions in the absence of one of the components or a combination of UBA1, Ub, and the respective E2 served as controls (#1–4). The E2 concentration present in sample #4 was equal to that in the reaction with the highest E2/UBA1 ratio (9, i.e., E1/E2 = 1:11). The reactions were incubated for 12 h at 37°C. Thereafter, reactions were stopped by cooling to 0°C. Following workup, the nucleotide species were analyzed by HPLC-HRMS. The $Ap_4A$ concentration that is present in commercially available ATP (measured in sample #1) was subtracted from the measured $Ap_4A$ concentrations. All data represent mean ± standard error of triplicates. Asterisks denote statistically non-significant values ($p > 0.05$) compared with #5, which served as control. All other results are statistically significant, i.e., $p < 0.05$ compared with #5. p values were determined by performing an unpaired t test in GraphPad Prism.

**$Ap_3A$ synthesis was much less efficient than $Ap_4A$ synthesis, and higher ADP concentrations (5 mM) interfered with E1 activity in general, preventing Ub-adenylate formation and, thus, also $Ap_nA$ synthesis. Therefore, we propose that E1 enzymes contribute only little to $Ap_3A$ formation.**

**Since the modification of proteins by the Ubl proteins NEDD8 and SUMO is significantly increased during stress conditions, we investigated whether the respective activating enzymes SAE and NAE are also able to generate $Ap_4A$. We found that the different E1 enzymes (UBA1, SAE, NAE) can all synthesize $Ap_4A$. The quantity of $Ap_4A$ formed, however, varied between the different E1 enzymes, with UBA1 being the most active one and SAE the least active one. Since the amount of AMP generated in the reactions was comparable, the observed differences in $Ap_4A$ synthesis are not attributable to different overall enzymatic activities. The differences may be explained by different accessibility of the Ubl-adenylate in the different E1 complexes. However, crystal structures allowing us to take a closer look at this possibility are not yet available.**

**Taken together, we discovered that $Ap_4A$ and, possibly, $Ap_3A$ are formed during Ub/Ubl activation in vitro. $Ap_4A$ and $Ap_3A$ are considered to be "alarmones" that signal cellular stress to evoke an intracellular response. Their precise functions, however, are only poorly understood, particularly in comparison with the intensively studied Ub/Ubl conjugation systems. Our results indicate for the first time the interdigitation of both signaling pathways.**

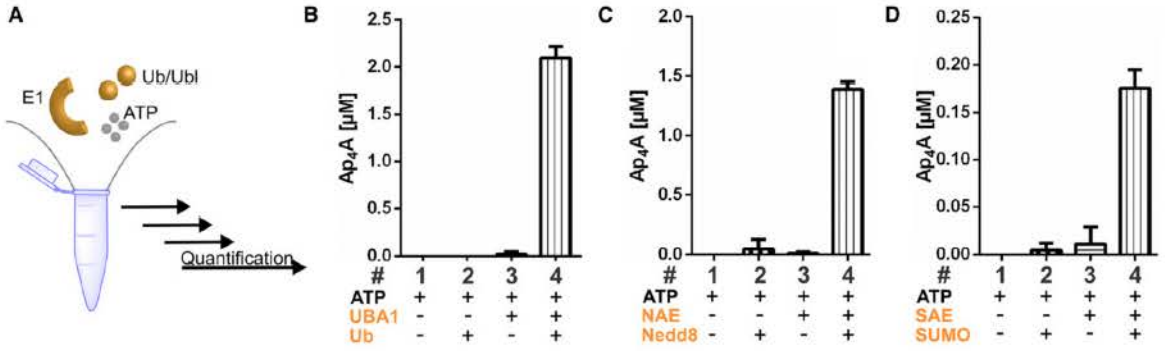


**Figure 6. $Ap_4A$ Synthesis by the E1 Enzymes for NEDD8 and SUMO**

(A) Comparison of the synthesis of $Ap_4A$ by Ub (B) with the Ubl systems, NAE (C) and SAE (D). The reaction mixture contained 0.8 µM E1, 60 µM Ubl, and 1 mM ATP in reaction buffer. Reactions, where E1 and/or Ubl were omitted, served as controls (#1–3). All reactions were incubated for 12 h at 37°C. Thereafter, the reactions were stopped by cooling to 0°C. After workup, the nucleotide species were analyzed by HPLC-HRMS. The $Ap_4A$ concentration, which is present in commercially available ATP (measured in sample #1), was subtracted from the measured $Ap_4A$ concentrations. All data represent mean ± standard error of triplicates.

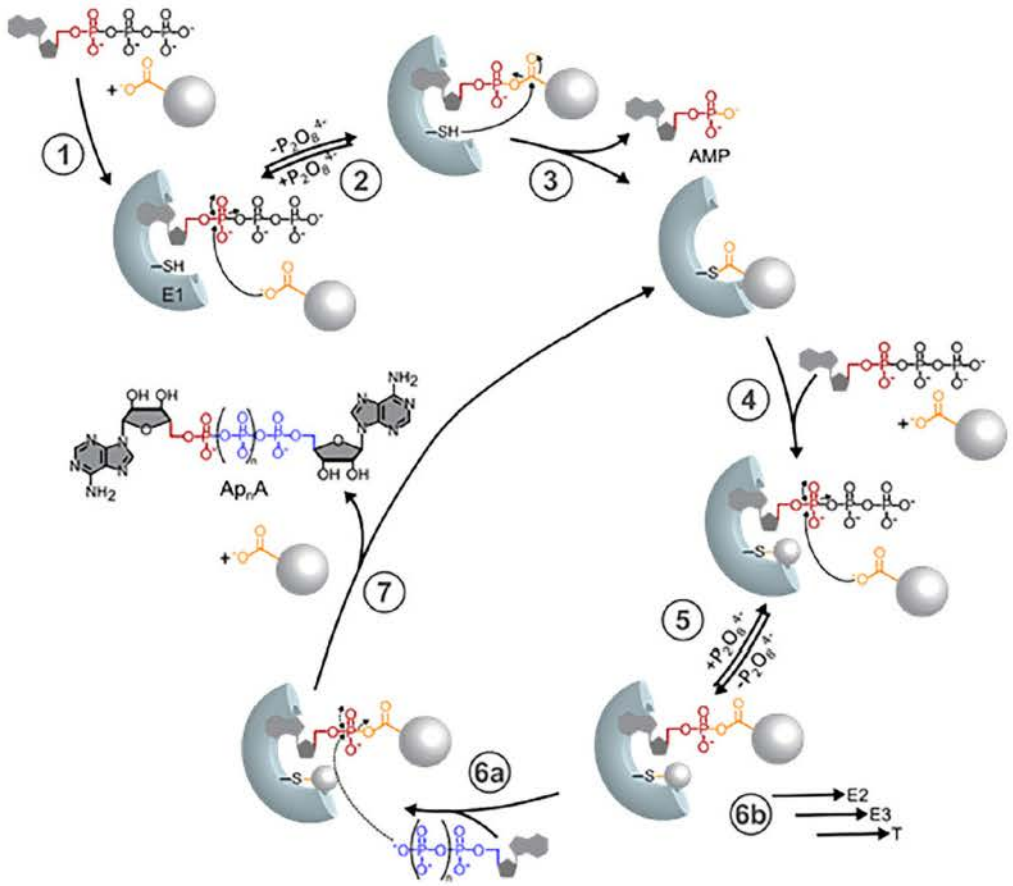


**Figure 7. Mechanistic Model for the Synthesis of $Ap_nA$ by the Ub/Ubl-Activating Enzyme E1**

First, Ub/Ubl is activated by its cognate E1 under consumption of ATP, forming a Ub/Ubl-adenylate (1 + 2). This adenylate is afterward attacked by the thiol group of the active-site cysteine, forming a thioester (3). The side reaction leading to the formation of $Ap_nA$ occurs after a second Ub/Ubl is adenylated by E1 (4 + 5). In $Ap_nA$ synthesis (6a), the adenylate is attacked by the phosphate group of an additional ADP/ATP (n = 1, 2) molecule, resulting in the formation of $Ap_3A$/$Ap_4A$ (n = 1, 2), respectively, and free Ub as well as E1-S-Ub can enter the catalytic cycle once more (7). In Ub/Ubl cascade (6b), the activated Ub/Ubl is transferred in a transthioesterification reaction to the Ub/Ubl-conjugating enzyme (E2). Next, the Ub/Ubl is ligated via a Ub/Ubl ligase (E3) to a Lys residue of the target protein (T), forming an isopeptide bond.


## ACKNOWLEDGMENTS

For financial support, we gratefully acknowledge the Deutsche Forschungsgemeinschaft (DFG) and the Konstanz Research School Chemical Biology.


## AUTHOR CONTRIBUTIONS

K.H.G., M.M., and A.M. conceived the project. K.H.G designed, optimized, and performed the biochemical experiments and purified all required enzymes except the Ub variants (Ub-His, Ub-R72A, Ub-LIA), which were cloned and purified by K.S. K.H.G and M.M. optimized and performed the HPLC-HRMS measurements. F.O. and M.S provided the bacterial strains for protein

expression as well as valuable input. K.H.G., M.M., and A.M. designed the experiments. K.H.G., M.S., and A.M. wrote the manuscript. All authors edited the manuscript.

## DECLARATION OF INTERESTS

The authors declare no competing interests.

## REFERENCES


Aiken, C.T., Kaake, R.M., Wang, X., and Huang, L. (2011). Oxidative stress-mediated regulation of proteasome complexes. Mol. Cell. Proteomics *10*, R110.006924.

Atencia, E.A., Madrid, O., Günther Sillero, M.A., and Sillero, A. (1999). T4 RNA ligase catalyzes the synthesis of dinucleoside polyphosphates. Eur. J. Biochem. *261*, 802–811.

Baker, J.C., and Jacobson, M.K. (1986). Alteration of adenyl dinucleotide metabolism by environmental stress. Proc. Nat. Acad. Sci. U S A *83*, 2350–2352.

Barnes, L.D., Garrison, P.N., Siprashvili, Z., Guranowski, A., Robinson, A.K., Ingram, S.W., Croce, C.M., Ohta, M., and Huebner, K. (1996). Fhit, a putative tumor suppressor in humans, is a dinucleoside 5′,5‴-P1,P3-triphosphate hydrolase. Biochem *35*, 11529–11535.

Baxi, M.D., and Vishwanatha, J.K. (1995). Diadenosine polyphosphates: their biological and pharmacological significance. J. Pharmacol. Toxicol. Methods *33*, 121–128.

Berndsen, C.E., and Wolberger, C. (2011). A spectrophotometric assay for conjugation of ubiquitin and ubiquitin-like proteins. Anal. Biochem. *418*, 102–110.

Bianchi, F., Tagliabue, E., Ménard, S., and Campiglio, M. (2007). Fhit expression protects against HER2-driven breast tumor development: unraveling the molecular interconnections. Cell Cycle *6*, 643–646.

Bohnsack, R.N., and Haas, A.L. (2003). Conservation in the mechanism of Nedd8 activation by the human AppBp1-Uba3 heterodimer. J. Biol. Chem. *278*, 26823–26830.

Brevet, A., Chen, J., Lévêque, F., Plateau, P., and Blanquet, S. (1989). In vivo synthesis of adenylylated bis(5′-nucleosidyl) tetraphosphates (Ap4N) by *Escherichia coli* aminoacyl-tRNA synthetases. Proc. Natl. Acad. Sci. U S A *86*, 8275–8279.

Burch, T.J., and Haas, A.L. (1994). Site-directed mutagenesis of ubiquitin. Differential roles for arginine in the interaction with ubiquitin-activating enzyme. Biochem *33*, 7300–7308.

Campiglio, M., Bianchi, F., Andriani, F., Sozzi, G., Tagliabue, E., Ménard, S., and Roz, L. (2006). Diadenosines as FHIT-ness instructors. J. Cell Physiol. *208*, 274–281.

Ciechanover, A. (1998). The ubiquitin-proteasome pathway: on protein death and cell life. EMBO J. *17*, 7151–7160.

Clemens, M.J. (2001). Initiation factor eIF2 alpha phosphorylation in stress responses and apoptosis. Prog. Mol. Subcell Biol. *27*, 57–89.

Dagmar, M., Beer, D.G., Wilke, C.W., Miller, D.E., and Glover, T.W. (1997). Frequent deletions of FHIT and FRA3B in Barretts metaplasia and esophageal adenocarcinomas. Oncogene *15*, 1653.

Farr, S.B., Arnosti, D.N., Chamberlin, M.J., and Ames, B.N. (1989). An apaH mutation causes AppppA to accumulate and affects motility and catabolite repression in *Escherichia coli*. Proc. Natl. Acad. Sci. U S A *86*, 5010–5014.

Finley, D., Ozkaynak, E., and Varshavsky, A. (1987). The yeast polyubiquitin gene is essential for resistance to high temperatures, starvation, and other stresses. Cell *48*, 1035–1046.

Flores, N.A., Stavrou, B.M., and Sheridan, D.J. (1999). The effects of diadenosine polyphosphates on the cardiovascular system. Cardiovasc. Res. *42*, 15–26.

Fontes, R., Günther Sillero, M.A., and Sillero, A. (1998). Acyl coenzyme a synthetase from pseudomonas fragi catalyzes the synthesis of adenosine 5′-polyphosphates and dinucleoside polyphosphates. J. Bacteriol. *180*, 3152–3158.

Fraga, H., and Fontes, R. (2011). Enzymatic synthesis of mono and dinucleoside polyphosphates. Biochim. Biophys. Acta *1810*, 1195–1204.

Garrison, P.N., Mathis, S.A., and Barnes, L.D. (1986). In vivo levels of diadenosine tetraphosphate and adenosine tetraphospho-guanosine in *Physarum polycephalum* during the cell cycle and oxidative stress. Mol. Cell Biol. *6*, 1179–1186.

Goerlich, O., Foeckler, R., and Holler, E. (1982). Mechanism of synthesis of adenosine(5′)tetraphospho(5′)adenosine (AppppA) by aminoacyl-tRNA synthetases. Eur. J. Biochem. *126*, 135–142.

Götz, K.H., Hacker, S.M., Mayer, D., Durig, J.N., Stenger, S., and Marx, A. (2017). Inhibitors of the diadenosine tetraphosphate phosphorylase Rv2613c of *Mycobacterium tuberculosis*. ACS Chem. Biol. *12*, 2682–2689.

Groen, E.J.N., and Gillingwater, T.H. (2015). UBA1: at the crossroads of ubiquitin homeostasis and neurodegeneration. Trends Mol. Med. *21*, 622–632.

Guo, R.-T., Chong, Y.E., Guo, M., and Yang, X.-L. (2009). Crystal structures and biochemical analyses suggest a unique mechanism and role for human glycyl-tRNA synthetase in Ap4A homeostasis. J. Biol. Chem. *284*, 28968–28976.

Hacker, S.M., Pagliarini, D., Tischer, T., Hardt, N., Schneider, D., Mex, M., Mayer, T.U., Scheffner, M., and Marx, A. (2013). Fluorogenic ATP analogues for online monitoring of ATP consumption: observing ubiquitin activation in real time. Angew. Chem. Int. Ed. *52*, 11916–11919.

Hendricks, D.T., Taylor, R., Reed, M., and Birrer, M.J. (1997). FHIT gene expression in human ovarian, endometrial, and cervical cancer cell lines. Cancer Res. *57*, 2112–2115.

Hershko, A., and Ciechanover, A. (1998). The ubiquitin system. Annu. Rev. Biochem. *67*, 425–479.

Huebner, K., Hadaczek, P., Siprashvili, Z., Druck, T., and Croce, C.M. (1997). The FHIT gene, a multiple tumor suppressor gene encompassing the carcinogen sensitive chromosome fragile site, FRA3B. BBA Rev. Cancer *1332*, M65–M70.

Impens, F., Radoshevich, L., Cossart, P., and Ribet, D. (2014). Mapping of SUMO sites and analysis of SUMOylation changes induced by external stimuli. Proc. Natl. Acad. Sci. U S A *111*, 12432–12437.

Karras, J.R., Paisie, C.A., and Huebner, K. (2014). Replicative stress and the FHIT gene: roles in tumor suppression, genome stability and prevention of carcinogenesis. Cancers *6*, 1208–1219.

Kerscher, O., Felberbaum, R., and Hochstrasser, M. (2006). Modification of proteins by ubiquitin and ubiquitin-like proteins. Annu. Rev. Cell Dev. Biol. *22*, 159–180.

Kisselev, L.L., Justesen, J., Wolfson, A.D., and Frolova, L.Y. (1998). Diadenosine oligophosphates (ApnA), a novel class of signalling molecules? FEBS Lett. *427*, 157–163.

Komander, D., and Rape, M. (2012). The ubiquitin code. Annu. Rev. Biochem. *81*, 203–229.

Leidecker, O., Matic, I., Mahata, B., Pion, E., and Xirodimas, D.P. (2012). The ubiquitin E1 enzyme Ube1 mediates NEDD8 activation under diverse stress conditions. Cell Cycle *11*, 1142–1150.

Lois, L.M., and Lima, C.D. (2005). Structures of the SUMO E1 provide mechanistic insights into SUMO activation and E2 recruitment to E1. EMBO J. *24*, 439–451.

Luthje, J., Baringer, J., and Ogilvie, A. (1985). Effects of diadenosine triphosphate (Ap3A) and diadenosine tetraphosphate (Ap4A) on platelet aggregation in unfractionated human blood. Blut *51*, 405–413.

Madrid, O., Martin, D., Atencia, E.A., Sillero, A., and Gunther Sillero, M.A. (1998). T4 DNA ligase synthesizes dinucleoside polyphosphates. FEBS Lett. *433*, 283–286.

Manfredi, G., Yang, L., Gajewski, C.D., and Mattiazzi, M. (2002). Measurements of ATP in mammalian cells. Methods *26*, 317–326.

Marriott, A.S., Copeland, N.A., Cunningham, R., Wilkinson, M.C., McLennan, A.G., and Jones, N.J. (2015). Diadenosine 5′,5′′-P(1),P(4)-tetraphosphate (Ap4A) is synthesized in response to DNA damage and inhibits the initiation of DNA replication. DNA Repair *33*, 90–100.

Marriott, A.S., Vasieva, O., Fang, Y., Copeland, N.A., McLennan, A.G., and Jones, N.J. (2016). NUDT2 disruption elevates diadenosine tetraphosphate (Ap4A) and down-regulates immune response and cancer promotion genes. PLoS One *11*, e0154674.

McLennan, A.G. (1992). Ap4A and Other Dinucleoside Polyphosphates, First Edition (CRC Press).

McLennan, A.G. (2000). Dinucleoside polyphosphates—friend or foe? Pharmacol. Ther. *87*, 73–89.

Mori, S., Shibayama, K., Wachino, J.-i., and Arakawa, Y. (2010). Purification and molecular characterization of a novel diadenosine 5′,5′′′-P1,P4-tetraphosphate phosphorylase from Mycobacterium tuberculosis H37Rv. Protein Expr. Purif. *69*, 99–105.

Mori, S., Shibayama, K., Wachino, J.-I., and Arakawa, Y. (2011). Structural insights into the novel diadenosine 5′,5‴-P1,P4-tetraphosphate phosphorylase from Mycobacterium tuberculosis H37Rv. J. Mol. Biol. *410*, 93–104.

Moris, G., Meyer, D., Orfanoudakis, G., Befort, N., Ebel, J.-P., and Remy, P. (1987). Dinucleoside tetraphosphate variations in cultured tumor cells during their cell cycle and growth. Biochem *69*, 1217–1225.

Mortensen, F., Schneider, D., Barbic, T., Sladewska-Marquardt, A., Kühnle, S., Marx, A., and Scheffner, M. (2015). Role of ubiquitin and the HPV E6 oncoprotein in E6AP-mediated ubiquitination. Proc. Natl. Acad. Sci. U S A *112*, 9872–9877.

Park, C.-W., and Ryu, K.-Y. (2014). Cellular ubiquitin pool dynamics and homeostasis. BMB Rep. *47*, 475–482.

Pichler, A., Gast, A., Seeler, J.S., Dejean, A., and Melchior, F. (2002). The nucleoporin RanBP2 has SUMO1 E3 ligase activity. Cell *108*, 109–120.

Plateau, P., and Blanquet, S. (1982). Zinc-dependent synthesis of various dinucleoside 5′,5′′′-P1,P3-Tri- or 5′,5′′′-P1,P4-tetraphosphates by *Escherichia coli* lysyl-tRNA synthetase. Biochem *21*, 5273–5279.

Proud, C.G. (2005). eIF2 and the control of cell physiology. Semin. Cell Dev. Biol. *16*, 3–12.

Rapaport, E., and Zamecnik, P.C. (1976). Presence of diadenosine -P1, P4-tetraphosphate (Ap4A) in mammalian cells in levels varying widely with proliferative activity of the tissue: a possible positive pleiotypic activator. Proc. Natl. Acad. Sci. U S A *73*, 3984–3988.

Ronau, J.A., Beckmann, J.F., and Hochstrasser, M. (2016). Substrate specificity of the ubiquitin and Ubl proteases. Cell Res. *26*, 441.

Saldivar, J.C., Shibata, H., and Huebner, K. (2010). Pathology and biology associated with the fragile FHIT gene and gene product. J. Cell Biochem. *109*, 858–865.

Schafer, A., Kuhn, M., and Schindelin, H. (2014). Structure of the ubiquitin-activating enzyme loaded with two ubiquitin molecules. Acta Crystallogr. D Biol. Crystallogr. *70* (Pt 5), 1311–1320.

Schneider, D., Schneider, T., Aschenbrenner, J., Mortensen, F., Scheffner, M., and Marx, A. (2016). Anionic surfactants enhance click reaction-mediated protein conjugation with ubiquitin. Bioorg. Med. Chem. *24*, 995–1001.

Shenton, D., Smirnova, J.B., Selley, J.N., Carroll, K., Hubbard, S.J., Pavitt, G.D., Ashe, M.P., and Grant, C.M. (2006). Global translational responses to oxidative stress impact upon multiple levels of protein synthesis. J. Biol. Chem. *281*, 29011–29021.

Siepmann, T.J., Bohnsack, R.N., Tokgöz, Z., Baboshina, O.V., and Haas, A.L. (2003). Protein interactions within the N-end rule ubiquitin ligation pathway. J. Biol. Chem. *278*, 9448–9457.

Sillero, A., and Sillero, M.A. (2000). Synthesis of dinucleoside polyphosphates catalyzed by firefly luciferase and several ligases. Pharmacol. Ther. *87*, 91–102.

Günther Sillero, M.A., de Diego, A., Silles, E., and Sillero, A. (2005). Synthesis of (di)nucleoside polyphosphates by the ubiquitin activating enzyme E1. FEBS Lett. *579*, 6223–6229.

Siprashvili, Z., Sozzi, G., Barnes, L.D., McCue, P., Robinson, A.K., Eryomin, V., Sard, L., Tagliabue, E., Greco, A., Fusetti, L., et al. (1997). Replacement of Fhit in cancer cells suppresses tumorigenicity. Proc. Natl. Acad. Sci. U S A *94*, 13771–13776.

Sorensen, M.A., Fehler, A.O., and Svenningsen, S.L. (2017). Transfer RNA instability as a stress response in *Escherichia coli*: rapid dynamics of the tRNA pool as a function of demand. RNA Biol. 586–593.

Sozzi, G., Tornielli, S., Tagliabue, E., Sard, L., Pezzella, F., Pastorino, U., Minoletti, F., Pilotti, S., Ratcliffe, C., Veronese, M.L., et al. (1997). Absence of fhit protein in primary lung tumors and cell lines with FHIT gene abnormalities. Cancer Res. *57*, 5207–5212.

Spasser, L., and Brik, A. (2012). Chemistry and biology of the ubiquitin signal. Angew. Chem. Int. Ed. *51*, 6840–6862.

Stewart, M.D., Ritterhoff, T., Klevit, R.E., and Brzovic, P.S. (2016). E2 enzymes: more than just middle men. Cell Res. *26*, 423–440.

Swatek, K.N., and Komander, D. (2016). Ubiquitin modifications. Cell Res. *26*, 399.

Thompson, D.M., Lu, C., Green, P.J., and Parker, R. (2008). tRNA cleavage is a conserved response to oxidative stress in eukaryotes. RNA *14*, 2095–2103.

Thorne, N.M., Hankin, S., Wilkinson, M.C., Nuñez, C., Barraclough, R., and McLennan, A.G. (1995). Human diadenosine 5′,5′′′-P1,P4-tetraphosphate pyrophosphohydrolase is a member of the MutT family of nucleotide pyrophosphatases. Biochem. J. *311* (Pt 3), 717–721.

Traut, T.W. (1994). Physiological concentrations of purines and pyrimidines. Mol. Cell Biochem. *140*, 1–22.

Varshavsky, A. (1983). Diadenosine 5′,5′′′-P1, P4-tetraphosphate: a pleiotropically acting alarmone? Cell *34*, 711–712.

Varshavsky, A. (2017). The ubiquitin system, autophagy, and regulated protein degradation. Ann. Rev. Biochem. *86*, 123–128.

Vartanian, A., Prudovsky, I., Suzuki, H., Dal Pra, I., and Kisselev, L. (1997). Opposite effects of cell differentiation and apoptosis on Ap3A/Ap4A ratio in human cell cultures. FEBS Lett. *415*, 160–162.

Vartanian, A., Alexandrov, I., Prudowski, I., McLennan, A., and Kisselev, L. (1999). Ap4A induces apoptosis in human cultured cells. FEBS Lett. *456*, 175–180.

Vartanian, A.A., Suzuki, H., and Poletaev, A.I. (2003). The involvement of diadenosine 5′,5′′′-P1,P4-tetraphosphate in cell cycle arrest and regulation of apoptosis. Biochem. Pharmacol. *65*, 227–235.

Verspohl, E.J., and Johannwille, B. (1998). Diadenosine polyphosphates in insulin-secreting cells: interaction with specific receptors and degradation. Diabetes *47*, 1727–1734.

Wang, X., Yen, J., Kaiser, P., and Huang, L. (2010). Regulation of the 26S proteasome complex during oxidative stress. Sci. Signal. *3*, ra88.

Weinmann-Dorsch, C., Hedl, A., Grummt, I., Albert, W., Ferdinand, F.-J., Friis, R.R., Pierron, G., Moll, W., and Grummt, F. (1984). Drastic rise of intracellular adenosine(5′)tetraphospho(5′)adenosine correlates with onset of DNA synthesis in eukaryotic cells. Eur. J. Biochem. *138*, 179–185.

Zamecnik, P.C., Stephenson, M.L., Janeway, C.M., and Randerath, K. (1966). Enzymatic synthesis of diadenosine tetraphosphate and diadenosine triphosphate with a purified lysyl-sRNA synthetase. Biochem. Biophys. Res. Commun. *24*, 91–97.

## KEY RESOURCES TABLE

| REAGENT or RESOURCE | SOURCE | IDENTIFIER |
|---|---|---|
| Bacterial and Virus Strain | | |
| E. coli BL21 CodonPlus (DE3)-RIL | Agilent | Cat#230240 |
| One shot BL21 (DE3) | Invitrogene | Cat#C600003 |
| BL834 (DE3) | | N/A |
| E.coli XL10 Gold | Agilent | Cat#200315 |
| E.coli NiCo BL21 (DE3) | New England Biolabs | Cat#C2529H |
| Chemicals, Peptides, and Recombinant Proteins | | |
| ATP magnesium-salt | Sigma-Aldrich, Merck | Cat#A9187 |
| ADP sodium salt | Sigma-Aldrich, Merck | Cat#A2754 |
| AMP sodium salt | Sigma-Aldrich, Merck | Cat#01930 |
| $Ap_3A$ (10 mM solution) | Jena Bioscience | Cat#NU-506 |
| $Ap_4A$( 10 mM solution) | Jena Bioscience | Cat#NU-507 |
| Ubiquitin from bovine erythrocytes | Sigma-Aldrich/ Merck | Cat#U6253 |
| NEDD8 E1 (NAE; APPBP1/UBA3) | Boston Biochem | Cat#E313 |
| NEDD8 | Boston Biochem | Cat#UL-812 |
| SUMO E1 (SAE; Aos1/UBA2) | This paper | N/A |
| SUMO | This paper | N/A |
| UBA1 | This paper | N/A |
| UBA1 C632S | This paper | N/A |
| Ub G76M | This paper | N/A |
| Ub LIA | This paper | N/A |
| Ub C-His | This paper | N/A |
| Ub R72A | This paper | N/A |
| UbcH5b | This paper | N/A |
| UbcH1 | This paper | N/A |
| Rv2613c | This paper | N/A |
| Critical Commercial Assays | | |
| NEBuilder HiFi DNA Assembly Master Mix | New England Biolabs | Cat#E2621 |
| Pierce TM BCA Protein Assay Kit | Thermo Fischer | Cat#23225 |
| Oligonucleotides | | |
| UBA1 C632S fragment for Gibson: TCAGGCACACTGGG CACCAAAGGCAATGTGCAGGTGGTGATCCCCTTCCTGACA GAGTCGTACAGTTCCAGCCAGGACCCACCTGAGAAGTCCA TCCCCATCTGTACCCTGAAGAACTTCCCTAATGCCATCGA GCACACCCTGCAGTGGGCTCGGGATGAATTTGAAGGCCTC TTCAAGCAGCCAGCAGAAAATGTCAACCAGTACCTCACAG ACCCCAAGTTTGTGGA | This paper synthesized by Integrated DNA Technologies | N/A |
| UBA1 C632S fwd Primer:TCAACCAGTACCTCACAGACCC | This paper, synthesized by Biomers | N/A |
| UBA1 C632S rev Primer: TGCACATTGCCTTTGGTGCCCA | This paper, synthesized by Biomers | N/A |
| Ub LIA (I44A) fwd Primer:GCAGCGTCTGGCTTTTGCAGGT AAACAGCTGGAA | This paper, synthesized by Biomers | N/A |
| Ub LIA (I44A) rev Primer: AAAGCCAGACGCTGCTGATCA GGCGGAATA | This paper, synthesized by Biomers | N/A |
| Ub LIA (L8A) fwd Primer: GTTAAAACCGCGACCGGTAAAA CCATTACA | This paper, synthesized by Biomers | N/A |
| Ub LIA (L8A) rev Primer: ACCGGTCGCGGTTTTAACAAAG ATCTGCAT | This paper, synthesized by Biomers | N/A |

(*Continued on next page*)

| *Continued* | | |
|---|---|---|
| REAGENT or RESOURCE | SOURCE | IDENTIFIER |
| Ub R72A fwd Primer: CATCTGGTTCTGGCTCTGCGTGG TGGTGTT | This paper, synthesized by Biomers | N/A |
| Ub R72A rev Primer: AACACCACCACGCAGAGCCAGAA CCAGATG | This paper, synthesized by Biomers | N/A |
| Recombinant DNA | | |
| pET32a_UBA1 | Berndsen and Wolberger, 2011 | N/A |
| pET32a_UBA1C632S | This paper | N/A |
| pET15b_Rv2613c wt | Götz et al., 2017 | N/A |
| pET28b_UBA2 | Pichler et al., 2002 | Addgene #53136 |
| pET28a-hAos1 | Pichler et al., 2002 | Addgene #53135 |
| pET11a_hSUMO1 | Pichler et al., 2002 | Addgene #53138 |
| pGEX2TK_UbG76M | Schneider et al., 2016 | N/A |
| pGEX2TK_Ub LIA | This paper | N/A |
| pGEX2TK_Ub R72A | This paper | N/A |
| pGEX2TK_Ub His | This paper | N/A |
| pET21a_UbcH5b | Mortensen et al., 2015 | N/A |
| pET21a_UbcH1 | Mortensen et al., 2015 | N/A |
| Software and Algorithms | | |
| QuantAnalysis 2.1 | Bruker | https://www.bruker.com/products/mr/mr-in-pharma/quantification.html |
| Graph Pad Prism 5 | Graphpad | https://www.graphpad.com/scientific-software/prism/ |
| Other | | |
| DNA sequencing | GATC/ Eurofins genomics | https://www.eurofinsgenomics.eu/de/custom-dna-sequencing/gatc-services/ |
| ZipTip C4® | Merck Millipore | ZTC04S008 |
| Deposited Raw Data for Figures 3, 4, and 5 | Deposited at Medeley data repository | https://doi.org/10.17632/g97kpmbvt3.1 |
| Deposited Raw Data for Figures 6, S1, and S2 | Deposited at Medeley data repository | https://doi.org/10.17632/xsgvjydt9y.1 |
| Deposited Raw Data for Figures S2–S6 | Deposited at Medeley data repository | https://doi.org/10.17632/wbpyfv76bs.1 |

## LEAD CONTACT AND MATERIALS AVAILABILITY

Further information and requests for resources and reagents should be directed to and will be fulfilled by the Lead Contact, Andreas Marx (Andreas.Marx@uni-konstanz.de).

## EXPERIMENTAL MODEL AND SUBJECT DETAILS

### *E. coli* Strains for Heterologous Expression

- BL21 Gold (DE3) (Genotype: F⁻ *ampT hsdS*($r_B^-$ $m_B^-$) *dcm*$^+$ Tet$^r$ *gal* λ(DE3) *end*A Hte, Stargene) cells were used for the expression of the E2 enzymes (UbcH5b, UbcH1), the Ub variants, the Ap4A phosphorylase ( Rv2613c) and SUMO1.
- CodonPlus BL21 (DE3) RIL (Genotype: F⁻ *ompT hsdS*($r_B^-$ $m_B^-$) *dcm*$^+$ Tet$^r$ *gal* λ (DE3) *end*A Hte [*argU ileY leuW* Cam$^r$]) cells were used for the expression of UBA1 and both subunits of SAE (UBA2/ Aos1).
- BL834 (DE3) (Genotype: F⁻ *ompT hsdS*$_B$($r_B^-$ $m_B^-$) *gal dcm met* (DE3), Novagene) cells were used for the expression of Ub G76M variant.
- NiCo BL21(DE3) (Genotype: *can*::*CBD fhuA2*[*lon*] *ompT gal* (λ *DE3*) [*dcm*] *arnA*::*CBD sylD*::*CBD glmS6Ala ΔhsdS* λ *DE3* = λ *sBamHIo ΔEcoRI-B int*::(*lacI*::*PlacUV5*::*T7 gene1*)*i21 Δnin5*, *New England Biolabs*) cells were used for the expression of the *inactive UBA1 C632S variant*.

### *E. coli* Strain Used for Cloning

- XL10 Gold (Genotype: Tet$^r$ Δ(*mcr*A)183 Δ(mcrCB-hsdSMR-mrr) 173 *end*A1 *sup*E44 thi-1 *rec*A1 *gyr*A96 *rel*A1 *lac* Hte [F' *pro*AB *lacI*$^q$ ZΔM15, Stargene) was used for transformation after molecular cloning.

## METHOD DETAILS

### Expression and Purification of Proteins

Human wild-type UBA1 was expressed as 6x-His-tagged protein from a pET32a vector in *E. coli* BL21(DE3)RIL cells as described (Berndsen & Wolberger, 2011). The human Ub–conjugating enzymes UbcH5b and UbcH1 were expressed as 6x-His-tagged protein from the pET21a vector in *E. coli* BL21 (DE3) cells as described (Mortensen et al., 2015). The diadenosine polyphosphate phosphorylase Rv2613c of *M. tuberculosis* was expressed from pET21a as a 6x-His-tagged protein as described (Götz et al., 2017; Mori et al., 2010).

#### *Generation of Expression Vector for UBA1C632S*

The UBA1 C632S variant was generated by Gibson assembly using the following cDNA (230 bp, purchased from IDT) TCAGGCA CACTGGGCACCAAAGGCAATGTGCAGGTGGTGATCCCCTTCCTGACAGAGTCGTACAGTTCCAGCCAGGACCCACCTGAGAAGTCCATCCCCATC TGTACCCTGAAGAACTTCCCTAATGCCATCGAGCACACCCTGCAGTGGGCTCGGGATGAATTTGAAGGCCTCTTCAAGCAGCCAGCAGAAAATGT CAACCAGTACCTCACAGACCCCAAGTTTGTGGA, which contained the desired mutation, and the linearized UBA wild-type cDNA in the pET32a vector, which lacks 165 bp were the cDNA is inserted. The vector was linearized by PCR with Phusion polymerase (New England Biolabs) according to the manufacturer's protocol. The following primers were used to introduce the C632A mutation and to linearize pET32a_UBA1 wt: 5'-d(TCA ACC AGT ACC TCA CAG ACC C) forward and 5'-d(TGC ACAT TGC CTT TGG TGC CCA) reverse. The PCR product was purified by 0.8% agarose gel followed by gel purification using the NucleoSpin® Gel and PCR Clean-up Kit (Macherey-Nagel). Vector and cDNA were assembled in a molar ratio of 1:2 using 2 x NEBuilder HiFi DNA Assembly Master Mix (New England Biolabs) in a total volume of 4 μL. The reaction mixture was incubated at 50°C for 20 min. After incubation, the whole reaction mixture was used for transformation of chemically competent *E.coli* XL10 Gold cells. The transformed cells were plated on agar plates containing the respective antibiotic and cultured overnight at 37°C. Single clones were picked and inoculated in LB medium containing carbenicillin (100 mg/L). After overnight incubation at 37°C, the plasmids were isolated with the QIAprep Spin Miniprep Kit (Qiagen) according to the manufacturer's instructions. The sequence was confirmed by Sanger sequencing (GATC).

#### *Expression of Human Recombinant UBA1 C632S*

UBA1 C632S was expressed as N-terminally-6x-His-tagged protein from the pET32a vector in *E. coli* NiCo BL21 (DE3) cells. Cells were grown overnight in LB medium containing carbenicillin (100 mg/L) at 37°C. The expression culture was inoculated to an $OD_{600}$ of 0.1 in LB medium containing carbenicillin (100 mg/L) and further incubated until an $OD_{600}$ of 0.6 was reached. Protein expression was induced by the addition of IPTG to a final concentration of 1.0 mM. Upon further incubation for 18 h at 20°C (160 rpm), cells were harvested by centrifugation (15 min, 4,400 g) at 4°C and the pellets were stored at -20°C or directly used for protein purification. For purification, the bacterial pellets were resuspended in 25 mL lysis buffer (1 x PBS, 1°%Triton X-100, 1 μg/mL Aprotinin / Leupeptin and 1 mg/mL Pefabloc®) on ice. Lysis was performed by sonication using a Bandelin MS72_sonotrode (duty cycle 30, Output control 0.25, 3 x 30 cycles) on ice. The lysate was cleared by centrifugation (38,760 g, 30 min) at 4°C. The supernatant was loaded onto a 1 mL His Trap FF crude column (GE Healthcare) pre-equilibrated with buffer containing 25 mM Tris-HCl pH 7.5, 300 mM NaCl and 10 mM imidazole. Bound protein was eluted with a linear gradient from 10 mM imidazole to 500 mM imidazole in 25 mM Tris-HCl, 300 mM NaCl, pH 7.5. Elution fractions were analyzed by SDS-PAGE followed by Coomassie blue staining. Fractions containing UBA1 C632S were concentrated in Vivaspin columns (50 kDa cutoff, Satorius), and the buffer was exchanged to 25 mM Tris-HCl pH 7.5, 300 mM NaCl, 1 mM DTT. UBA1 C632S was further purified by size exclusion chromatography (25 mM Tris-HCl pH 7.5, 300 mM NaCl and 1 mM DTT) on a Sephadex 200 column (120 mL volume). Elution fractions were analyzed by SDS-PAGE followed by Coomassie blue staining, pooled and the buffer was exchanged to 25 mM Tris-HCl pH 7.5, 50 mM NaCl containing 50% (v / v) glycerol. Protein concentration was determined by NanoDrop™ ND-1000 (peQLab Biotechnology). Aliquots were stored at -20°C.

#### *Expression of Ub Variants*

The G76M mutant of human ubiquitin was expressed as GST-tagged protein from the pGEX2TK vector in *E. coli* BL834 (DE3) cell as described (Schneider et al., 2016).

The codon optimized cDNA of Ub with a C-terminal 6x-His-tag was inserted into the pGEX 2TK backbone, but with the GST cDNA deleted to yield pKS Ub-His. The LIA (L8A, I44A) and R72A mutations were generated by site-directed mutagenesis to yield pKS Ub LIA -His and pKS Ub R72A -His. The following primers were used: I44A 5''-d(GCA GCG TCT GGC TTT TGC AGG TAA ACA GCT GGA AG) forward, 5'-d(AAA GCC AGA CGC TGC TGA TCA GGC GGA ATA) reverse; L8A 5'-d(GTT AAA ACC GCG ACC GGT AAA ACC ATT ACA) forward, 5'-d(ACC GGT CGC GGT TTT AAC AAA GAT CTG CAT) reverse; R72A 5'-d(CAT CTG GTT CTG GCT CTG CGT GGT GGT GTT) forward, 5'-d(AAC ACC ACC ACG CAG AGC CAG AAC CAG ATG) reverse. *E.coli* BL21(DE3) cells containing the corresponding pKS vector were grown overnight (37°C, 180 rpm, LB medium containing 100 mg/L carbenicillin). The expression culture was inoculated to an $OD_{600}$ of 0.1 in LB medium containing carbenicillin (100 mg/L) and further incubated (37°C, 220 rpm) until an $OD_{600}$ of 0.7 was reached. IPTG was added to a final concentration of 1 mM to induce protein expression. After incubation for 6h (37°C, 220 rpm), cells were harvested by centrifugation (10 min, 4,400 g) at 4°C. The bacterial pellets were resuspended in lysis buffer (50 mM Tris-HCl, 150 mM NaCl, 30 mM imidazole, pH 7.4, 1 mg/ml Aprotinin / Leupeptin, 1 mg/mL Pefabloc®) and lysed by sonication. The lysate was cleared by centrifugation (39,000 x g, 4°C, 30 min) and the Ub -His variants were purified using a 5 mL HisTrap HP (Äkta pure25) with a linear gradient from 30 mM imidazole to 500 mM imidazole in 50 mM Tris-HCl, 150 mM NaCl, pH 7.4 for elution. Fractions containing Ub -His variants were pooled and either dialyzed directly or UBP core (Ronau et al., 2016) was added to remove the C-terminal His-tag before dialysis. Dialysis (3.5K MWCO, Thermo Fischer Scientific) was performed against 25 mM Tris-HCl pH 7.5, 50 mM NaCl overnight at room temperature. The samples were then diluted 1:3 with 25 mM NaOAc pH 4.5 and

purified using a 1 mL HiTrap SP HP (Äkta pure 25) and a gradient from 0-1 M NaCl in 25 mM NaOAc pH 4.5. Fractions containing the Ub variants were were analyzed by SDS-PAGE followed by Coomassie blue staining, pooled, dialyzed against 25 mM Tris-HCl pH 7.5, 50 mM NaCl and concentrated using Amicon Ultra (3 kDa MWCO). The concentration was determined with the Pierce™ BCA Protein Assay Kit (Thermo Fischer Scientific) according to the manufacturer's instructions and commercial Ub (Ub from bovine erythrocytes, Merck) as standard.

***Expression of Human Recombinant SAE***

The two subunits (Aos1 / UBA2) of SAE were expressed separately as 6x-His-tagged proteins in *E. coli* and the active heterodimer was subsequently reconstituted. The expression vectors pET28a-Aos1 and pET28b-UBA2 were purchased from addgene (#53135, #53136) and were originally constructed in the lab of F. Melchior, Heidelberg (Pichler et al., 2002). Both vectors were separately transformed into competent BL21 (DE3) RIL cells, expression and purification of both subunits was performed alike. The cells were grown overnight in LB medium supplemented with 0.1 % (w / v) glucose, 1.0 mM $MgCl_2$, kanamycin (34 mg/L) and chloramphenicol (34 mg/L) at 37°C. The expression culture was inoculated to an $OD_{600}$ of 0.1 in LB medium supplemented with 0.1 % (w / v) glucose, 1.0 mM $MgCl_2$ and the respective antibiotics, and further incubated (37°C, 160 rpm) until an $OD_{600}$ of 0.6 was reached. Protein expression was induced by addition of IPTG to a final concentration of 1.0 mM and the cultures were further incubated for 18 h at 25°C (160 rpm). Then, cells were harvested by centrifugation (15 min, 4,400 g) at 4°C and the pellets were stored at -20°C or directly used for protein purification. To do so, the bacterial pellets were resuspended in 25 mL lysis buffer (50 mM Tris-HCL pH 7.5, 100 mM NaCl, 1 µg/mL Aprotinin / Leupeptin and 1 mg/mL Pefabloc®) on ice. Lysis was performed by sonication using a Bandelin MS72_sonotrode (duty cycle 30, Output control 0.25, 3 x 30 cycles) on ice. The lysates were cleared by centrifugation (38,759 g, 30 min) at 4°C. The supernatant was loaded onto a 1 mL His Trap FF crude column (GE Healthcare) that was pre-equilibrated with buffer containing 50 mM Tris-HCl pH 7.5, 100 mM NaCl, 1.0 mM DTT and 10 mM imidazole. The protein was eluted by a linear gradient from 10 mM imidazole to 500 mM imidazole in 50 mM Tris-HCl, 100 mM NaCl, 1.0 mM DTT pH 7.5. The elution fractions were analyzed by SDS-PAGE and Coomassie blue staining. Fractions containing the respective subunit were concentrated in Amicon ultra centrifugal filters (10 kDa cutoff, Merck), and the buffer was exchanged to 20 mM HEPES pH 7.3, 110 mM KOAc, 2.0 mM $MgCl_2$, 1.0 mM EDTA and 1 mM DTT. Both subunits were further purified by size exclusion chromatography (20 mM HEPES pH 7.3, 110 mM KOAc, 2.0 mM $MgCl_2$, 1.0 mM EDTA and 1 mM DTT, HiLoad™ 16/60 Superdex™ 75, prep grade). Elution fractions containing protein were analyzed by SDS-PAGE and Coomassie blue staining, pooled and concentrated using Amicon ultra centrifugal filters (10 kDa cutoff, Merck). The protein concentration was determined with the Pierce™ BCA Protein Assay Kit (Thermo Fischer Scientific) according to the manufacturer's instructions. To reconstitute the dimeric SUMO E1 (SAE), His-Aos and Uba2-His were combined in equimolar concentrations on ice overnight. To separate the complex from excess non-dimerized subunits, size exclusion chromatography was performed (20 mM HEPES pH 7.3, 110 mM KOAc, 2.0 mM $MgCl_2$, 1.0 mM EDTA and 1 mM DTT; GE Healthcare, HiLoad™ 16/60 Superdex™ 200, prep grade). Elution fractions containing protein were analyzed by SDS-PAGE and Coomassie blue staining and pooled accordingly. The reconstituted SAE was concentrated and the buffer was exchanged to 50 mM Tris-HCl pH 7.5, 100 mM NaCl, 1.0 mM DTT and 10 % (v / v) glycerol using Amicon ultra centrifugal filters (10 kDa cut off, Merck). Protein concentration was determined by SDS-Page followed by Coomassie blue staining in comparison to a BSA standard. 10 µL aliquots were frozen in liquid $N_2$ and stored at −20°C.

***Expression of Human Recombinant SUMO***

The expression vector pET11a-SUMO1 was purchased from addgene (#53138) and was originally constructed in the lab of Frauke Melchior (Pichler et al., 2002). The plasmid was transformed into chemically competent *E. coli* cells (BL21 Gold). A single colony was inoculated into LB medium containing carbenicillin (100 mg/L) and grown at 37°C (160rpm) overnight. The expression culture was inoculated to an $OD_{600}$ of 0.1 in LB medium containing carbenicillin (100 mg/L) and further incubated (37°C, 160 rpm) until an $OD_{600}$ of 0.6 was reached. Protein expression was induced by the addition of 1.0 mM IPTG (final concentration) and the culture further incubated for 4 h at 37°C (160 rpm). Then, cells were harvested by centrifugation (15 min, 4,400 g) at 4°C and the pellet was stored at −20°C or directly used for protein purification. For this purpose, the bacterial pellet was resuspended in 25 mL lysis buffer (25 mM Tris-HCl pH 8.0, 50 mM NaCl, 1.0 mM DTT, 1 µg/mL Aprotinin / Leupeptin and 1 mg/mL Pefabloc®) on ice. Lysis was performed by sonication using a Bandelin MS72_sonotrode (duty cycle 30, Output control 0.25, 3 x 30 cycles) on ice. The lysate was cleared by centrifugation (38,759 g, 30 min) at 4°C. The supernatant was loaded onto a 1 mL HiTrap Q column (GE Healthcare) pre-equilibrated with buffer containing 25 mM Tris-HCl pH 8.0, 50 mM NaCl, 1.0 mM DTT. The protein was eluted by a linear gradient from 50 mM NaCl to 500 mM NaCl in 25 mM Tris-HCl pH 8.0, 1.0 mM DTT. The elution fractions were analyzed by SDS-PAGE and Coomassie blue staining. Fractions containing SUMO1 were concentrated in Vivaspin columns (3 kDa cutoff, Satorius), and the buffer was exchanged to 25 mM Tris-HCl pH 7.5, 300 mM NaCl, 1 mM DTT. SUMO1 was further purified by size exclusion chromatography (25 mM Tris-HCl pH 7.5, 300 mM NaCl and 1 mM DTT; HiLoad™ 16/60 Sephadex™ 75, prep grade). Elution fractions containing protein were analysed by SDS-PAGE and Coomassie blue staining, pooled and the buffer was exchanged to 25 mM Tris-HCl pH 7.5, 50 mM NaCl containing 10 % (v / v) glycerol. Protein concentration was determined with the Pierce™ BCA Protein Assay Kit (Thermo Fischer Scientific) according to the manufacturer's instructions. Aliquots were frozen in liquid $N_2$ and stored at −20°C.

**E1-$Ap_nA$ Assay**

The respective E1 enzyme (UBA1, SAE, NAE) was mixed with its cognate Ubl and ATP in a buffer containing 25 mM Tris-HCl pH 7.6, 50 mM NaCl, 5 mM $MgCl_2$, 1.25 mM DTT in a total volume of 20 µL on ice. When indicated, E2 enzymes (UbcH1, UbcH5b) were added as well. The concentrations of all components are indicated in the respective experiments. Reaction mixtures were incubated at 37°C overnight. After incubation, the samples were put on ice, and the proteins were removed using $ZipTip_{C4}$® pipette tips (see Sample

Purification). Thereafter, the samples were diluted with 500 μL water, frozen in liquid nitrogen and lyophilized. Then, samples were centrifuged for one minute at full speed in a table top centrifuge to collect all of the content at the bottom of the reaction tube. The white powder was solved in 30 μL water. To ensure complete solubilization, samples were incubated for 5 min at 37°C with shaking at 600 rpm. The samples were frozen in liquid nitrogen or directly analyzed by HPLC-HRMS (see MS Analysis and Quantification of $Ap_nA$).

#### *Sample Purification*

$ZipTip_{C4}$ pipette tips (Merck Millipore) are 10 μL pipette tips with a bed volume of 0.6 μL reversed-phase chromatography resin fixed at its ends. First the resin was wetted by repeated (ten times) dispensing and aspiration of wetting solution ($H_2O$ : MeCN 1 : 1). To achieve maximum binding of proteins, the media was then equilibrated in water containing 0.1% TFA by repeated washing (ten times). For the removal of proteins 10 μL of the reaction sample were added and then aspirated and dispensed twenty times, to allow binding of the to the resin. Finally, bound proteins were eluted from the resin by aspirating and dispensing ten times in 10 μL of elution solution (75 % MeCN, 0.1 % TFA in water). The tip was reused and equilibration and protein binding steps were repeated with the remaining 10 μL of the sample.

### MS Analysis

#### *MS Analysis of $Ap_nA$ Assay*

20 μL of a given sample (see E1-$Ap_nA$ assay) were separated on a 100*2.1 Hypercarb® column (Thermo Fisher Scientific) with a gradient of 10 mM $NH_4Ac$ pH 10 (solvent A) and MeCN (solvent B) each supplemented with 0.1 % diethylamine (gradient 5% B to 25% B over 5 min, 25% B to 35% B over 15 min). For regeneration the column was washed with 100% B followed by equilibration in 5% B at a flow rate of 300 μL/min.

MS measurements were performed on a micrOTOF II (Bruker) in negative mode using a mass range of 300 to 900 m/z. 2x rolling average was used and spectra were recorded at a frequency of 1 Hz. Mass accuracy was assured by calibration using ammonium formate clusters as internal standard. (For further Data Analysis see Quantification of $Ap_nA$).

#### *Determination of Detection Limit of $Ap_nA$*

20 μL of samples with a different $Ap_3A$ and $Ap_4A$ (mixture of both) concentration (0.01 μM, 0.1μM, 0.5 μM, 1.0 μM) were separated on a 100*2.1 Hypercarb® column (Thermo Fisher Scientific) with a gradient of 10 mM $NH_4Ac$ pH 10 (solvent A) and MeCN (solvent B) each supplemented with 0.1% diethylamine (gradient 5% B to 25% B over 5 min, 25% B to 35% B over 15 min). For regeneration the column was washed with 100% B followed by equilibration in 5% B at a flow rate of 300 μL/min.

MS measurements were performed on a micrOTOF II (Bruker) in negative mode using a mass range of 300 to 900 m/z. 2x rolling average was used and spectra were recorded at a frequency of 1 Hz. Mass accuracy was assured by calibration using ammonium formate clusters as internal standard. (For further Data Analysis see Quantification of $Ap_nA$).

## QUANTIFICATION AND STATISTICAL ANALYSIS

### Quantification of $Ap_nA$

In order to obtain reliable quantitative information, prior to the measurement of each series of samples a standard curve was generated by measuring seven different concentrations of both $Ap_3A$ and $Ap_4A$ (0.1 μM, 0.25 μM, 0.5 μM, 1.0 μM, 2.5 μM, 5 μM, and 10 μM in 20 μL volume). Processing of data was performed using QuantAnalysis 2.1 (Bruker). First, extracted ion chromatograms with a width of +/- 0.1 were created. Then, the relevant peaks in the chromatograms were integrated and quantified according to the corresponding standard curve.

For the quantification of AMP, a standard curve was generated by measuring six different concentrations (0.5 μM, 1.0 μM, 2.5 μM, 5 μM, 10 μM and 20 μM in 20 μL volume). Processing of data was performed using QuantAnalysis 2.1 (Bruker). First, extracted ion chromatograms with a width of +/- 0.1 were created. Then, the relevant peaks in the chromatograms were integrated and quantified according to the corresponding standard curve.

As detection limit (compare Determination of Detection Limit of $Ap_nAs$ by MS) 2 pmol were determined (20 μL 100 nM solution). Till this concentration $Ap_3A$ and $Ap_4A$ were detectable with a signal to noise ratio greater than 3.

### Statistical Analysis

For all experiments, N = 3 biological replicates were examined for each condition. Statistical parameters (p) were calculated by GraphPad Prism using an unpaired t-test (Version 5 Graphpad) and are reported in the figures when values were similar.

## DATA AND CODE AVAILABILITY

The raw datasets (i.e., from HPLC-HRMS runs) supporting the current study are deposited at the Mendeley Data repository (see Key Resource Table for details).